JOURNAL OF THERMOPHYSICS AND HEAT TRANSFER
Vol. 22, No. 4, October–December 2008

Equilibrium Properties of High-Temperature Air for a Number of Pressures

Sean J. Henderson* and James A. Menart†
Wright State University, Dayton, Ohio 45440

DOI: 10.2514/1.36141

This paper presents compositions and thermodynamic properties for air in chemical equilibrium for a number of pressures and a range of temperatures. The temperature range of interest is from 300 to 30,000 K and the pressures covered are 1×10^{-6}, 1×10^{-4}, 1×10^{-2}, 1, and 100 atm. Twenty-two species that can result from an original mixture of 21% O_2, 78% N_2, and 1% Ar are included in the analysis. The equilibrium composition is presented in terms of mole fractions. The thermodynamic properties presented are the constant-pressure specific heat, specific enthalpy, specific entropy, molecular-weight ratio, ratio of specific enthalpy to specific internal energy, ratio of frozen specific heats, ratio of equilibrium specific heats, and the isentropic index. Because a number of other investigators have obtained equilibrium-air properties over the years, another objective of this work is to make comparisons with these results. These comparisons are important so that the reader can see where the results agree and where they differ. The results presented here cover a wider range of conditions than those presented elsewhere for properties that are important for analyzing high-speed flight conditions.

Nomenclature

a	=	polynomial curve-fit coefficient
a_i	=	moles of i element in the gas mixture or curve-fit coefficient
C_P	=	specific heat at constant pressure, J/kg · K
$C_\mathcal{V}$	=	specific heat at constant volume, J/kg · K
$C_P^\circ(T)$	=	molar specific heat at constant pressure of a chemical species, J/mol · K
c	=	speed of sound, m/s
e	=	specific internal energy, J/kg
g_m	=	degeneracy of mth electronic energy level
g_j°	=	molar Gibbs free energy of individual chemical species, J/mol
h	=	specific enthalpy, J/kg
$h^\circ(T)$	=	molar enthalpy of a chemical species, J/mol
I	=	ionization energy, J
k_b	=	Boltzmann constant (1.38×10^{-23} J/K)
$\mathcal{M}$	=	molecular weight, kg/mol
$\mathcal{M}_o$	=	molecular weight of undissociated gas, kg/mol
$\mathcal{N}_a$	=	Avogadro's number (6.023×10^{23}/mol)
$\mathcal{N}_i$	=	moles of species i
$\mathcal{N}_{\text{tot}}$	=	total moles of gas mixture
NE	=	number of elements
NS	=	number of species
n_{ij}	=	number of elements i in a species j particle
P	=	pressure, Pa
Q	=	molecular partition function
R	=	specific gas constant, J/kg · K
R_o	=	specific gas constant of undissociated air (286.99 J/kg · K)
$\Re$	=	universal gas constant (8314 J/mol · K)
S_c	=	Sackur–Tetrode constant (1.164856)
s	=	entropy, J/kg · K
$s^\circ(T)$	=	molar entropy of a chemical species, J/mol · K
T	=	temperature, K
$\mathcal{V}$	=	volume, m^3
X	=	mole fractions
Z	=	ratio of molecular weights
$\mathcal{Z}$	=	neutral atom or molecule
$\Delta H_f^\circ(T)$	=	enthalpy of formation of a single ion, molecule, or electron, J
$\Delta h_f^\circ(T)$	=	enthalpy of formation, J/mol
ϵ_m	=	energy of the mth electronic energy level, J
γ	=	ratio of specific heats (C_p/C_v)
γ_s	=	isentropic exponent
$\bar{\gamma}$	=	ratio of enthalpy over internal energy
λ_i	=	element potential of element i
ρ	=	density, kg/m^3

Subscripts

eq	=	equilibrium
fr	=	frozen
i	=	element
m	=	gas mixture
n	=	degree of ionization

I. Introduction

TO ACCURATELY determine the correct hydrodynamic and thermal characteristic of the flowfield around an aircraft moving at hypersonic speeds, it is necessary that accurate properties of the gas be determined. At Mach numbers below 4 to 5, air is essentially composed of 79% diatomic nitrogen and 21% diatomic oxygen, which can be used to determine the required thermodynamic properties with good accuracy. However, for higher-speed flows, the air starts to disassociate and ionize due to the higher temperatures. This change in composition can have large effects on the properties of the gaseous medium and thus affect the predicted hydrodynamic and thermal fields calculated using computational fluid dynamics [1].

There are three goals of the work presented here: The first goal is to expand the range of thermodynamic properties for air that are available in the literature by producing a computational routine that will predict accurate thermodynamic properties as a function of temperature and pressure and include the effects of composition change. The second goal is to compare these results with those

Presented as Paper 2159 at the 35th AIAA Plasmadynamics and Lasers Conference, Portland, OR, 28 June–1 July 2004; received 10 December 2007; revision received 9 July 2008; accepted for publication 13 July 2008.

*Ph.D. Student, Department of Mechanical Engineering. Member AIAA.
†Associate Professor, Department of Mechanical Engineering. Member AIAA.

published by a number of other investigators [2–6]. This provides readers with an idea of the accuracy of the results presented in this paper and an idea of the accuracy of the results presented by other investigators. The third goal is to present what may be called gamma parameters for temperatures over 20,000 K. The gamma values include the ratio of specific enthalpy to specific internal energy, the ratio of frozen specific heats, the ratio of equilibrium specific heats, and the isentropic index. These parameters are useful in some computational fluid dynamic codes. It seems the gamma values have only been presented in the literature up to 20,000 K. All of them are presented up to 30,000 K in this work for a pressure of 1×10^{-4} atm and 1 atm.

It is known that there are a number of software programs that exist for determining the equilibrium composition of air. To name a few of the more popular equilibrium-composition programs, there is the popular CHEMKIN-II program, the NASA CEA [7–9] code for the calculation of complex chemical equilibrium compositions, the popular STANJAN [10] program of Stanford University that uses the element potential method, and the PEGASE [11] code of the von Karman Institute. There are also a large number of published results for the thermodynamic properties of equilibrium air that were not included due to space constraints. Even though this is the case, there is still room for more published data on high-temperature properties of air, especially at lower pressures. This is needed in this day and age, in which hypersonic aircraft are being seriously researched.

The composition and thermodynamic properties of equilibrium air as presented in the literature are calculated using somewhat different techniques. There are three techniques used to determine the equilibrium composition of air: the equilibrium constant method [12–15], the minimization of Gibbs free-energy method [14], and the element potential method [10]. All three of these techniques can provide exact results, but the equilibrium constant method requires knowledge of each of the chemical reactions occurring, whereas the minimization of the Gibbs free-energy method and the element potential method only require knowledge of the species produced and each of the elements in the reaction. For this reason, the element potential method is used in this work.

Some of the differences in the models used by different investigators that cause differences in the results are the number of species included, the thermodynamic data used for the individual species, and whether or not the Debye correction or the second virial correction is used. The Debye correction takes into account the long-range interactions between charged particles. The virial correction takes into account the interaction potential of the particles as they approach each other. In addition, the forms in which the thermodynamic results are presented vary from researcher to researcher, with the most common forms being tabulated data [3,6], graphical data [4], and curve fits [2,5]. As part of this work, a number of comparisons are made with the works of the researchers shown in Table 1.

II. CANTERA Program

The particular program used in this work to perform the required calculations is called CANTERA [16]. CANTERA is an open-source, object-oriented software package for problems involving chemically reacting flows developed and maintained by the Division of Engineering and Applied Science at the California Institute of Technology. To use the CANTERA suite of software, a user interface must be written. This user interface can be written in a number of languages that include FORTRAN, PYTHON, MATLAB, and C^{++}. Because FORTRAN is a CPU-time-efficient computer language, the user interface required for this project was written in FORTRAN. All user interfaces to CANTERA use a common C^{++} kernel. All but the C^{++} interface use a C interface library.

Results from CANTERA were compared with those from the popular software CHEMKIN-II [17]. The results obtained from these two sets of software were identical to several significant figures, but CANTERA took less than one-third the computational time. Computational speed was an important consideration in the writing of CANTERA. Property caching is used so that expensive reaction rates are only computed when the temperature changes. Virtual methods are used sparingly, inlining is allowed, and because the source code is available, other optimization techniques can be implemented.

III. Species Property Determination

In this work, the element potential method is used to determine the equilibrium composition of the gas. The element potential method requires knowledge of the thermodynamic properties of the individual species present in the gas mixture. For this reason, the thermodynamic properties of all the species present in the products have to be found before the equilibrium composition can be found. The fundamental data needed to determine the equilibrium composition and thermodynamic properties of the gas are the molar specific heat at constant pressure C_p°, molar enthalpy h°, and molar entropy s° of each chemical species that is included in the products. These data have to be known as a function of temperature. For the 22 species of interest in this work (N_2, O_2, Ar, O, N, NO, N_2^+, O_2^+, NO^+, N^+, N^{+2}, N^{+3}, O^+, O^{+2}, O^{+3}, Ar^+, Ar^{+2}, Ar^{+3}, N^-, O^-, O_2^- and e^-), this was done for the temperature range from 300 to 30,000 K.

The thermodynamic properties of the individual molecular species for the temperature range from 300 to 20,000 K and the individual monatomic atoms for the range from 300 to 6000 K were obtained from publications by the NASA John H. Glenn Research Center at Lewis Field (GRC) [18,19]. These publications provide the thermodynamic data for over 2000 chemical species. The thermodynamic properties provided are h°, s°, and C_p° as a function of temperature using polynomials with 9 coefficients. The thermodynamic properties of the individual species can also be obtained from GRC [20]. The 9 coefficient polynomial forms provided by GRC are of the form

$$\frac{C_P^\circ(T)}{\Re} = \frac{a_1}{T^2} + \frac{a_2}{T} + a_3 + a_4 T + a_5 T^2 + a_6 T^3 + a_7 T^4 \qquad (1)$$

$$\frac{h^\circ(T) - h^\circ(298.15)}{\Re T} = -\frac{a_1}{T^2} + \frac{a_2 \ell_n(T)}{T} + a_3 + \frac{a_4 T}{2} + \frac{a_5 T^2}{3} + \frac{a_6 T^3}{4} + \frac{a_7 T^4}{5} + \frac{b_1}{T} \qquad (2)$$

Table 1 Equilibrium air models

Researcher(s)	Included species	Corrections[a]	Curve fit
Present work	O_2, O, O^+, O^{+2}, O^{+3}, O_2^+, O^-, O_2^-, N_2, N, N^+, N^{+2}, N^{+3}, N_2^+, N^-, NO, NO^+, Ar, Ar^+, Ar^{+2}, Ar^{+3}, e^-	No	No
Gupta [2]	O_2, O, O^+, O^{+2}, N_2, N, N^+, N^{+2}, NO, NO^+, e^-	No	Yes
Boulos [3]	O_2, O, O^+, O^{+2}, O_2^+, N_2, N, N^+, N^{+2}, N_2^+, NO, NO_2, N_2O, NO^+, Ar, Ar^+, Ar^{+2}, e^-	Yes	No
Hansen [4]	O_2, O, O^+, N_2, N, N^+, e^-	No	No
Srinivasan [5]	O_2, O, O^+, N_2, N, N^+, NO, NO^+, e^-	No	Yes
Hillensrath and Klein [6]	O_2, O, O^+, O^{+2}, O_2^+, O^-, O_2^-, N_2, N, N^+, N^{+2}, N_2^+, N^-, NO, NO^+, NO_2, N_2O, Ar, Ar^+, Ar^{+2}, C, C^+, C^{+2}, CO, CO_2, CO^+, Ne, Ne^+, e^-	Yes	No

[a]Debye and virial corrections.

$$\frac{s^\circ(T)}{\Re} = -\frac{a_1}{2T^2} - \frac{a_2}{T} + a_3\,\ell_n(T) + a_4 T + \frac{a_5 T^2}{2} + \frac{a_6 T^3}{3} + \frac{a_7 T^4}{4} + b_2 \tag{3}$$

It should be noted that the enthalpy of formation is given relative to the reference temperature of 298.15 K. These 9 coefficient polynomials need to be altered because CANTERA uses 7 coefficient polynomials [21]. The 7 coefficient polynomials required by CANTERA are of the form

$$\frac{C_P^\circ(T)}{\Re} = a_0 + a_1 T + a_2 T^2 + a_3 T^3 + a_4 T^4 \tag{4}$$

$$\frac{h^\circ(T) - h^\circ(298.15)}{\Re T} = a_0 + \frac{a_1 T}{2} + \frac{a_2 T^2}{3} + \frac{a_3 T^3}{4} + \frac{a_4 T^4}{5} + \frac{a_5}{T} \tag{5}$$

$$\frac{s^\circ(T)}{\Re} = a_0\,\ell_n T + a_1 T + \frac{a_2 T^2}{2} + \frac{a_3 T^3}{3} + \frac{a_4 T^4}{4} + a_6 \tag{6}$$

In these 6 equations, a are the desired coefficients, T is the temperature, and $\Re$ is the universal gas constant. We have transformed the 9 coefficient data provided by GRC to the 7 coefficient form required by CANTERA by using a least-squares fit. This was done for the given temperature range with a maximum difference in the two types of correlations of less than 3%. For the most part, the conversion was done with a difference of less than 1%.

The thermodynamic properties for all the monatomic atoms and ions were calculated using partition functions for the temperature range from 6000 to 30,000 K. The reason for this is that GRC [18,19] only provides thermodynamic properties up to 20,000 K. Diatomic species are not included in the analysis past 20,000 K, because it can be shown from the equilibrium-composition results that they are almost completely disassociated at these high temperatures. The reason for calculating the partition functions from 6000 to 30,000 K for monatomic species was that the thermodynamic properties obtained from the literature were compared with the thermodynamic data of GRC [19] at 20,000 K, and a slight difference could be seen in the values of h°, s°, and C_P°. However, when our data obtained from partition functions were compared with the data of GRC at 6000 K, there was excellent agreement. With this approach, an erroneous jump in the mole fractions and thermodynamic properties of the air is not seen at 20,000 K.

The code used to obtain the partition functions for the monatomic species and their thermodynamic properties was the NASA code PAC99, which was also developed by GRC. A brief description of the capabilities of the code is given by McBride and Gordon [7] and Gordon and McBride [19]. PAC99 calculates the internal partition functions for monatomic gases from the following equation:

$$Q = \left(\sum_{m=1}^{\infty} g_m e^{-\epsilon_m / k_b T} \right)^{N_a} \tag{7}$$

where g_m and ϵ_m are the degeneracy and electronic excitation energy for the mth energy level of the single atom or ion. This equation also involves two constants: the Boltzmann constant k_b and Avagradro's number N_a. Avagradro's number is included in this equation to convert the molecular partition function to the canonical partition function for 1 mol of gas or plasma [22]. To obtain the partition function, the electronic energy levels of the monatomic species are required, along with the associated degeneracies. This information can easily be obtained from the NIST Atomic Spectra Database [23]. This work does not fill in energy levels that are missing in the National Institute of Standard and Technology (NIST) database, as was done in the work of Capitelli et al. [24]. The lowering of the ionization potential is accounted for using the Temper technique [19].

Once the internal canonical partition functions are calculated, the thermodynamic functions C_p°, h°, and s° can be calculated as

$$\frac{C_p^\circ(T)}{\Re} = T^2 \frac{\mathrm{d}^2(\ell_n Q)}{\mathrm{d}T^2} + \frac{5}{2} \tag{8}$$

$$\frac{h^\circ(T) - h^\circ(0)}{\Re T} = T \frac{\mathrm{d}(\ell_n Q)}{\mathrm{d}T} + \frac{5}{2} \tag{9}$$

$$\frac{s^\circ(T)}{\Re} = T \frac{\mathrm{d}(\ell_n Q)}{\mathrm{d}T} + \ell_n Q + \frac{3}{2}\ell_n \mathcal{M} + \frac{5}{2}\ell_n T + S_c \tag{10}$$

where $\mathcal{M}$ is the molecular weight, and S_c is the Sackur–Tetrode constant, which has a value of 1.164856 when using 1 atm as the standard pressure.

Once the thermodynamic functions are calculated using Eqs. (9) and (10) for the temperature range of interest, a least-squares fit of the data is performed to fit the data to the 7 coefficient polynomials shown in Eqs. (4–6). The only additional piece of information needed to calculate the thermodynamic properties are the enthalpies of formation at 298.15 K. The arbitrary base of having the enthalpy of formation $\Delta h_f^\circ(298.15)$ and molar enthalpy $h^\circ(298.15)$ equal to each other at a temperature of 298.15 K is used to account for the chemical energy present in the molecules. This information can be found either in the GRC data [7,18,19] or by using the following equation for the case of ions:

$$\Delta H_{f,\mathcal{Z}^{n+1}}^\circ(298.15) = \Delta H_{f,\mathcal{Z}^n}^\circ(298.15) + I_{\mathcal{Z}^n} - \Delta H_{f,e^-}^\circ(298.15) \tag{11}$$

where $\Delta H_{f,\mathcal{Z}^n}^\circ$ is the enthalpy of formation of a single particle of the species being ionized, and $\Delta H_{f,\mathcal{Z}^{n+1}}^\circ$ is the enthalpy of formation of the ionized species. The neutral species being ionized is $\mathcal{Z}$, the degree of ionization of the species being ionized is n, the ionization energy required to ionize the species is $I_{\mathcal{Z}^n}$, and the enthalpy of formation of an electron is $\Delta H_{f,e^-}^\circ$.

IV. Determining the Equilibrium Composition

For the dry-air calculations being performed in this paper, the concentrations of 22 different species are determined as a function of pressure and temperature. The 22 species, which will be called the number of species (NS), are determined as a result of combinations of breaking apart 3 different elements: N, O, and Ar. The number of these elements will be called NE. When these elements are broken apart, an electron and a positive ion are formed. There is one electron formed for every single ion formed, two electrons for every double ion, and three electrons for every triple ion.

The following section will give a short description of how the element potential method is used for determining the equilibrium composition of an ideal-gas mixture. For a more detailed derivation and explanation of the element potential method, Reynolds [10] can be consulted. To aid in the discussion that follows, the mole fractions X_i and specific gas constant R are defined as

$$X_i = \frac{\mathcal{N}_i}{\sum_{i=1}^{\mathrm{NS}} \mathcal{N}_i} \quad \text{and} \quad R_m = \sum_{i=1}^{\mathrm{NS}} \frac{\mathcal{R}}{X_i \mathcal{M}_i} \tag{12}$$

where $\mathcal{M}_i$ is the molecular weight of the chemical species i, and $\mathcal{N}_i$ is the number of moles of species i in the gas mixture.

The element potential method and minimization of Gibbs free-energy method both are derived from a fundamental law: the second law of thermodynamics. The minimization of Gibbs free energy involves minimizing the Gibbs free energy of NS species with conservation of mass as a constraint. The element potential method involves the minimization of NE element potentials λ_i, with conservation of mass as a constraint. In a gas mixture with a large number of species present, there are a smaller number of elements

present, and so the system of equations to be solved simultaneously is smaller for the element potential method.

The molar Gibbs free energy g_j° of chemical species j can be determined from h_j° and s_j° that are supplied as input data to the CANTERA program for each chemical species present in the gas mixture:

$$g_j^\circ = h_j^\circ - s_j^\circ T \tag{13}$$

The conservation of mass can be written as an atomic population constraint:

$$\sum_{j=1}^{\mathrm{NS}} n_{ij}\mathcal{N}_j = a_i \qquad i = 1, 2, \ldots, \mathrm{NE} \tag{14}$$

where n_{ij} is the number of elements i in species j, and a_i is the moles of element i present in the gas mixture.

In summary, the element potential is found by trying to minimize the Gibbs free energy by taking arbitrary variations of the quantity of each element. With some algebraic manipulation and the use of the conservation-of-mass constraint, the mole fractions can be expressed as a function of element potentials and the Gibbs free energies. For every species, we have

$$X_j = \exp\left(\frac{-g_j^\circ}{\Re T} + \sum_{i=1}^{\mathrm{NE}} \lambda_i n_{ij}\right) \tag{15}$$

The element potentials of the elements, λ_i, are actually Lagrange multipliers. The method of Lagrange multipliers is used to minimize the Gibbs free energy with the conservation-of-mass constraint.

Substituting the mole fractions determined in Eq. (15) into the conservation-of-mass equation (14) means that the element potentials can be determined by

$$\sum_{j=1}^{NS} n_{ij}\mathcal{N}_{\mathrm{tot}}X_j = \sum_{j=1}^{\mathrm{NS}} n_{ij}\mathcal{N}_{\mathrm{tot}} \exp\left(\frac{-g_j^\circ}{\Re T} + \sum_{i=1}^{\mathrm{NE}} \lambda_i n_{ij}\right) = a_i \qquad i = 1, 2, \ldots, \mathrm{NE} \tag{16}$$

From the definition of mole fractions, we have

$$\sum_{j=1}^{\mathrm{NS}} X_j = \sum_{j=1}^{\mathrm{NS}} \exp\left(\frac{-g_j^\circ}{\Re T} + \sum_{i=1}^{\mathrm{NE}} \lambda_i n_{ij}\right) = 1 \tag{17}$$

With Eqs. (16) and (17), we have NE + 1 equations that must be solved simultaneously to determine the element potentials. Once the element potentials are determined, the mole fractions can easily be found using Eq. (15). With a good initial guess of the mole fractions of the dominant species in the gas mixture, a form of the Newton–Raphson method can be used to solve the system of equations.

V. Gas-Mixture Property Determination

Once the thermodynamic properties of the individual species are found, the thermodynamic properties of the gas mixture can be determined using ideal-gas-mixture rules, as discussed in many references [2,12,13].

For this work, all species are assumed to be an ideal gas. There is virtually no error introduced into the properties for the species of interest for temperatures above 300 K and pressures below 1 atm. The three mixture properties are all on a per-mass basis. These properties are internal energy e_m, enthalpy h_m, and entropy s_m, which are determined from

$$h_m = \sum_{i=1}^{\mathrm{NS}} \frac{X_i h_i^\circ}{\mathcal{M}_m} \tag{18}$$

$$e_m = h_m - RT \tag{19}$$

$$s_m = \sum_{i=1}^{\mathrm{NS}} \frac{X_i s_i^\circ}{\mathcal{M}_m} - R\sum_{i=1}^{\mathrm{NS}} \ell n(X_i) - R\,\ell n\left(\frac{P}{P_\circ}\right) \tag{20}$$

where the subscript m refers to the property value for the product mixture, and P_o is the reference pressure of 1 atm.

The total specific heat at constant pressure and the total specific heat at constant volume, which are a combination of the frozen and reactional contributions, can be determined from

$$C_{P,m} = \left.\frac{\partial h_m}{\partial T}\right|_P \quad \text{and} \quad C_{V,m} = \left.\frac{\partial e_m}{\partial T}\right|_{\mathcal{V}} \tag{21}$$

For a gas in chemical equilibrium, the ratio of enthalpy over internal energy $\bar{\gamma}$ is often used in computational fluid dynamics codes. It is defined as

$$\bar{\gamma} = \frac{h_m}{e_m} \tag{22}$$

where it should be noted that the mixture enthalpy and internal energy are taken as their absolute values and not from their reference states. With the use of $\bar{\gamma}$, the following relationship between pressure, density, and internal energy can be obtained:

$$P = (\bar{\gamma} - 1)\rho e \tag{23}$$

Equation (23) is almost identical to the perfect-gas relation for pressure, except that $\bar{\gamma}$ is replaced with the ratio of frozen specific heats for the perfect-gas case. In fact, at lower temperatures, $\bar{\gamma}$ converges to the ratio of specific heats.

The speed of sound is obtained from its definition as

$$c^2 = \left(\frac{\partial P}{\partial \rho}\right)_s \tag{24}$$

For a frozen perfect-gas mixture, the equation for the frozen speed of sound is

$$c_{\mathrm{fr}} = \sqrt{\gamma_{\mathrm{fr}} R_m T} \tag{25}$$

where γ_{fr} is the ratio of frozen specific heats, and R is the specific gas constant of the gas.

There are several forms in which the equilibrium speed of sound can be expressed as a function of the ratio of the equilibrium specific heats γ_{eq}, but the simplest expression is very similar to the frozen speed of sound using the isentropic exponent γ_s. Using the isentropic exponent, the equilibrium speed of sound can be cast in the following form [9,25]:

$$c_{\mathrm{eq}} = \sqrt{\gamma_s RT} \tag{26}$$

where

$$\gamma_s = \frac{\gamma_{\mathrm{eq}}\rho}{P}\left(\frac{\partial P}{\partial \rho}\right)_T$$

The equation of state for an equilibrium gas can be defined as

$$P = Z\rho R_o T \tag{27}$$

where $Z = \mathcal{M}_o/\mathcal{M}$, and where $\mathcal{M}_o$ is the molecular weight of the undissociated gas, $\mathcal{M}$ is the average molecular weight of the equilibrium gas, and Z is the ratio of the molecular weights. It should be mentioned that the ratio of molecular weights is commonly referred to as the compressibility factor in the high-temperature-gas literature. This can be misleading terminology, because the compressibility factor is also used to show the deviation of a real gas from an ideal gas. In this work, all gases are ideal and Z simply accounts for the changing molecular weight.

VI. Results

In this work, air is assumed to be composed of 21% diatomic oxygen, 78% diatomic nitrogen, and 1% argon at room temperature. At elevated temperatures, these three fundamental species are allowed to react into the following 22 species: N_2, O_2, Ar, O, N, NO, N_2^+, O_2^+, NO^+, N^+, N^{+2}, N^{+3}, O^+, O^{+2}, O^{+3}, Ar^+, Ar^{+2}, Ar^{+3}, N^-, O^-, O_2^-, and e^-. Included in this list of 22 species are diatomic molecules, monotonic molecules, positive ions, negative ions, and free electrons. This is a fairly inclusive list for temperatures below 30,000 K. Because of the highly variable nature of the water vapor content in atmospheric air, this is not included in the analysis. It is typical to leave this component out in air-composition calculations.

A. Equilibrium-Composition Results

To verify the results of the equilibrium composition, the mole fractions of this work are compared with mole fractions from Hillsenrath and Klein [6] at pressures of 1×10^{-6} and 1 atm for a temperature range of 1000 to 15,000 K. These results, as well as results from this work, up to 30,000 K are shown in Figs. 1 and 2. Figures 1a and 2a present the mole fractions of the neutral species, and Figs. 1b and 2b present the mole fractions of the ionized species. The neutral and ionized species mole fractions were split into two figures for easier viewing. Hillsenrath and Klein have the most detailed model of all of the results with which comparisons are made in this work. Hillensrath and Klein's equilibrium-air model uses 29 species and includes Debye and second virial corrections. Hillensrath and Klein also include the species NO_2, N_2O, C, C^+, C^{+2}, CO, CO_2, CO^+, Ne, and Ne^+, which are not included in this work. These species are only present in trace amounts (mole fractions less than 5×10^{-4}) for the range of temperatures and pressures given by Hillensrath and Klein, and are therefore not shown in Figs. 1 and 2. This work includes the species O^{+3}, N^{+3}, and Ar^{+3}, which are not included by Hillensrath and Klein. These species do not affect Hillensrath and Klein's compositions, because they only provide results up to 15,000 K; triply ionized species do not start to appear in significant amounts for temperatures less than 20,000 K for the range of pressures of interest.

Figure 1a shows excellent agreement between the mole-fraction results of the present work and those of Hillensrath and Klein [6] for all of the neutral species. Hillensrath and Klein show slightly lower mole fractions for argon at lower temperatures, but this is due to C and Ne being included in their model, and therefore they specified the initial mole fraction of Ar to be slightly lower than is specified in this work. Figure 1b shows excellent agreement between the mole-fraction results for all of the ionized species.

Figure 2a presents the mole fractions of the neutral species at 1 atm, and Fig. 2b presents the mole fractions of the ionized species at 1 atm. For the mole fractions of the neutral species, we see that there is excellent agreement between all of the species. The slight discrepancy between the mole fractions of Ar at lower temperatures is again due to the different initial mole fractions specified in the two models. For the mole fractions of the ionized species at 1 atm, we see that there is excellent agreement between the mole fractions for the

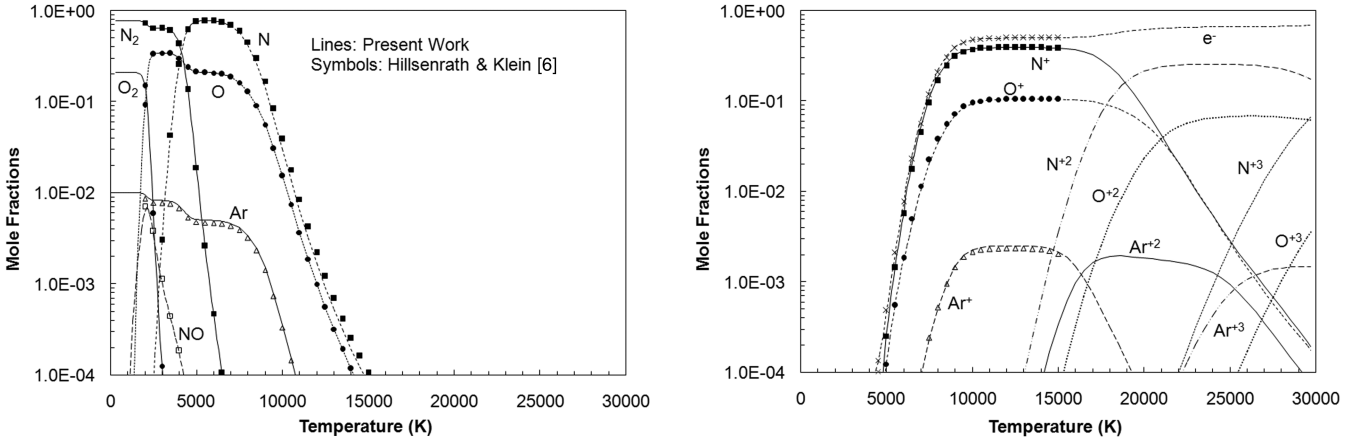

a) Neutral species b) Ionized species

Fig. 1 Mole fractions at 1×10^{-6} atm.

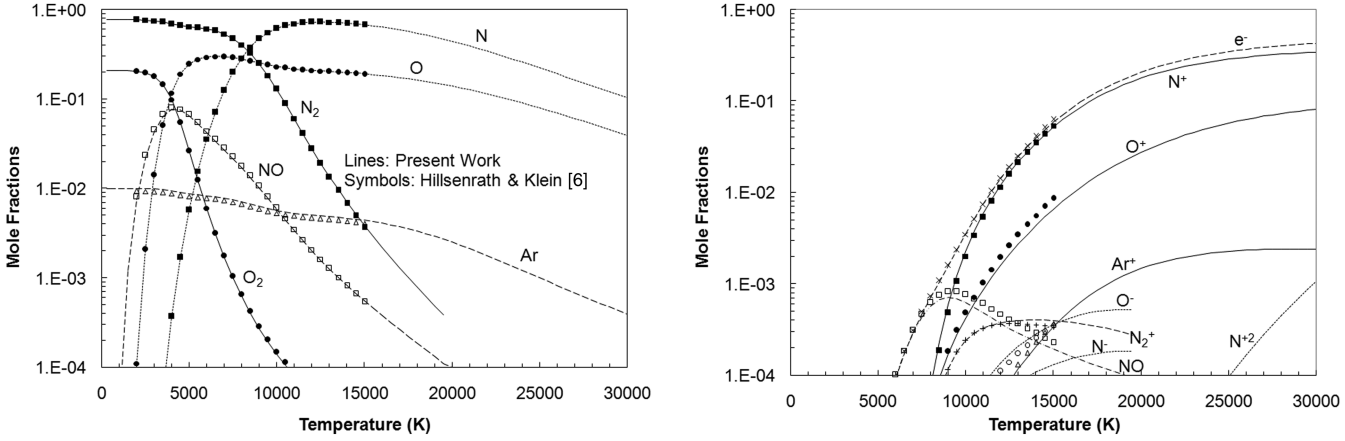

a) Neutral species b) Ionized species

Fig. 2 Mole fractions at 1 atm.

species of N^+ and Ar^+; however, the agreement between the mole fractions of the species of O^+, N_2^+, NO^+, O^-, and N^- is not as good. This is probably due to inaccuracies that existed in the partition functions of diatomic and negative ions at higher temperatures ($\sim T > 10,000$ K) in Hillensrath and Klein's [6] work. The partition functions used in calculating the thermodynamic properties by Hillensrath and Klein were obtained during the 1960s, and the partition functions obtained for this work were recently obtained from GRC [20] and NIST [23]. These databases are frequently updated for what are viewed as the most accurate values of the energy levels. In addition, more energy levels are added to the databases as they become available. We thus believe that more accurate partition functions are used in this work than those used by Hillensrath and Klein [6]. The reason these differences do not show up at lower pressures such as 1×10^{-6} atm, as shown in Fig. 1b, is due to the fact that diatomic species dissociate at lower temperatures for lower pressures. Thus, the diatomic species do not have a chance to ionize in significant amounts at lower pressures, because they disassociate before a high-enough temperature is reached for ionization. This same trend can be seen for ionization of monatomic atoms and ions; they ionize at lower temperatures as the pressure is decreased.

For all the pressures surveyed, the dominant species at the lower temperatures are N^2 and O^2. For the middle range of temperatures, the dominant species are N, O, and NO. For the higher temperatures, N^+, O^+, and electrons are the dominant species. At still higher temperatures, N^{+2}, O^{+2}, and electrons become the dominant species, with N^{+3} and O^{+3} starting to become important above 25,000 K for lower pressures. The double and triply ionized species become more important at lower temperatures as the pressure decreases. In fact, N^{+2} and O^{+2} become more dominant than N^+ and O^+ at temperatures higher than 15,000 K for lower pressures. The species NO is important in the range of temperatures from 1000 to 8000 K, depending on the pressure. Argon is only 1% of the mixture at 300 K and it drops from there as other particles are formed and neutral argon becomes ionized. The negative-ion species and the positive-ion diatomic molecules are never a significant percentage of the total number of particles. These species can be important if looking at the electrical properties of the gas at low temperatures.

B. Thermodynamic Property Results

The thermodynamic property results of this work are compared with the results of Gupta et al. [2], Boulos et al. [3], Hansen [4], and Srinivasan et al. [5]. Boulos et al.'s [3] results are obtained from the most detailed model. Boulos et al.'s model contains 18 species and uses Debye and second virial corrections. Boulos et al.'s model, however, does not include triply ionized species and only present's results at 1 atm for temperatures up to 24,000 K. The second most detailed model is that of Gupta et al. [2], which uses 11 air species and uses spliced polynomial curve fits to present the thermodynamic results. The Gupta et al. model also does not include triply ionized species, but presents results up to 30,000 K. The third most detailed model is Srinivasan et al. [5], which uses a 9-species air model and also uses spliced polynomial curve fits. The Srinivasan et al. model does not include either double or triply ionized species and presents results to $\sim$20,000 K. The least detailed model is Hansen [4], which includes 7 species from air, but does not include double or triply ionized species, NO, and NO^+.

For the comparison of the mixture enthalpies for equilibrium air, the results are presented as nondimensional enthalpies for four different pressures in Fig. 3a. The enthalpy is nondimensionalized by dividing the enthalpy by the specific gas constant of the undissociated air, $R_o = 286.99$ J/kg · K, and the temperature. For all three of the presented pressures, the enthalpies of the various models show excellent agreement with the results of this work. The results of Gupta et al. [2] and Srinivasan et al. [5] have enthalpies that tend to oscillate above and below the enthalpies of the present work. This is due to the spliced polynomial curve fits used by these investigators.

For comparisons of the mixture entropies for equilibrium air, the results are presented in nondimensional form for three different pressures, as shown in Fig. 3b. The entropy is nondimensionalized by dividing by R_o. The entropy results of Hansen [4] and Srinivasan et al. [5] show excellent agreement to the entropy results of this work. The results of Srinivasan et al. again show some oscillation about the entropy results of the present work, due to the spliced polynomial curve fits.

The molecular-weight ratios of Fig. 4a show excellent agreement between all of the models for all pressures. For the minor differences that appear between the molecular-weight ratios obtained by other investigators and the results of this work, the same reasoning discussed with the enthalpies applies.

For comparisons of the mixture specific heats at constant pressure for equilibrium air, the results are also presented in nondimensional form for three different pressures, as shown in Fig. 4b. The specific heat at constant pressure is nondimensionalized by dividing $C_{P,m}$ by R_o. The results of Hansen [4] and Gupta et al. [2] show excellent agreement with the results of this work, except for the upper temperature range of these models. Looking at the $C_{P,m}$ results of Hansen [4], it can seen that the results of Hansen show $C_{P,m}$ leveling off at 13,000 K at a pressure of 1×10^{-4} atm, whereas the results of this work show $C_{P,m}$ starting to increase. The reason for this difference is that Hansen does not include doubly ionized species in his model; double ionized species start to become important at about 13,000 K for a pressure of 1×10^{-4} atm. This same leveling-off behavior can be seen when comparing the results of Gupta et al. [2] with the results of this work at 24,000 K for 1×10^{-4} atm and 27,000 K for 1×10^{-2} atm. These differences are due to Gupta et al.

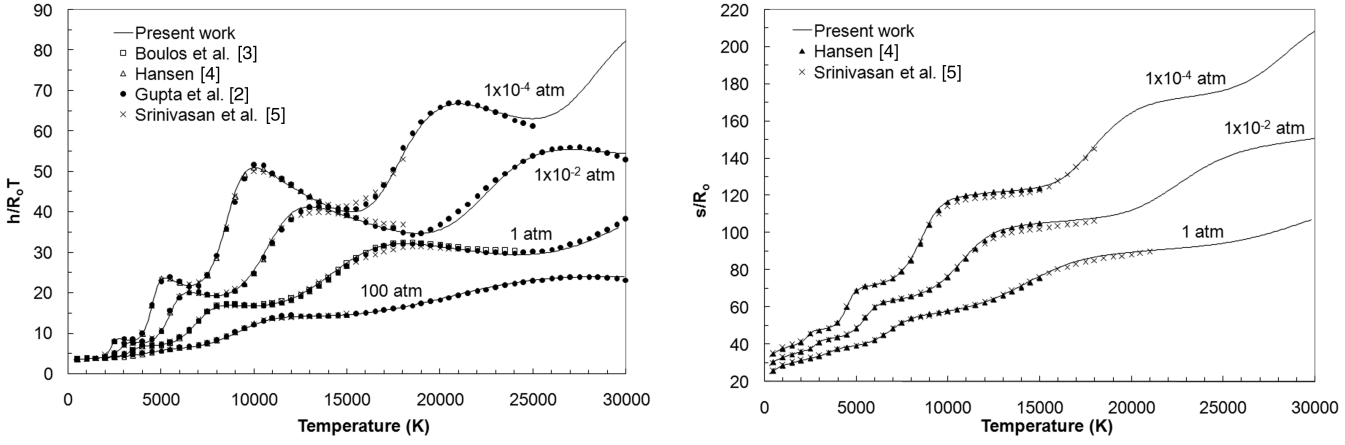

a) Nondimensional enthalpy

b) Nondimensional entropy

Fig. 3 Comparison of enthalpy and entropy at various pressures.

neglecting triply ionized species in their model. The triply ionized species start to significantly ionize at these temperatures and pressures.

Looking at Figs. 3a and 4a for the specific enthalpy, specific entropy, and molecular-weight ratio, it can be seen that there are certain temperature regions in which these properties change rapidly and other regions in which these properties level off. The rapid changes are due to the disassociation of the molecules and ionization of the species. The effects of disassociation and ionization can be seen most drastically in the total specific heat at constant-pressure results (see Fig. 4b). The large humps in these results correspond to rapid changes in the enthalpy. These are the regions in which disassociation and ionization are occurring in a strong way. The first hump corresponds to disassociation of O_2, the second hump corresponds to disassociation of N_2, the third hump corresponds to ionization of O and N, the fourth hump corresponds to the ionization of N^+ and O^+, and the fifth hump corresponds to the ionization of N^{+2} and O^{+2}. It should be noted that the enthalpy also has regions in which it levels off. In addition, Fig. 3a shows the nondimensional enthalpy decreasing in certain regions. It should be noted that the dimensional enthalpy is actually constant or increasing slightly in these regions; the nondimensional enthalpy shows a drop because it is divided by the temperature.

Figure 5 shows the comparisons of all the gamma parameters with the results of Hansen [4] and Srinivasan et al. [5] for pressures of 1×10^{-4} and 1 atm. Looking at Fig. 5, we can see that γ_{fr}, γ_{eq}, and γ_s all converge to the same value for temperatures less than 3000 K. This shows that the frozen-specific-heat assumption is good for low temperatures, and only a single gamma parameter is needed. The $\bar{\gamma}$ parameter converges to γ_{fr} around room temperature. Comparing the γ_{fr} and γ_{eq} parameters, it can be seen that γ_{fr} is larger than γ_{eq} for temperatures greater than 3000 K. This occurs because γ_{eq} takes into account the chemical reactions occurring in equilibrium air. We can also see that γ_{eq} and γ_s follow the same pattern, with both having large humps. These large humps correspond to regions in which dissociation and ionization are occurring, and the different peaks are the same as those discussed with the enthalpy. From the comparison of the γ_{eq} results of Hansen [4] with this work, we see that the results show excellent agreement for 1 atm and 1×10^{-4} atm for temperatures up to 13,000 K. The reason for the disagreement at higher temperatures is that Hansen does not include doubly ionized species in his model. The agreement of the isentropic exponent γ_s between the results of Hansen [4] and Srinivasan et al. [5] and this work is good for lower temperatures, but only fair for higher temperatures. Determining the isentropic index involves the calculation of the derivative $(\partial P/\partial \rho)|_T$, which is difficult to do. This derivative changes drastically because the density varies wildly with changes in pressure, especially at higher temperatures. This means that a slight difference in density is magnified in the isentropic exponent. The agreement of $\bar{\gamma}$ between the results of Srinivasan et al. and the present work is excellent for both pressures. Finally, looking at Fig. 5, we can see that the gamma parameters are functions of both temperature and pressure, and the different gamma values can be significantly different at all but the lowest temperatures.

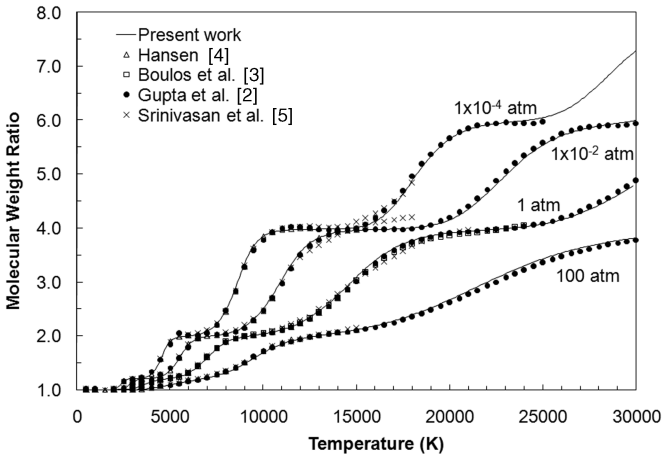

a) Molecular weight ratio

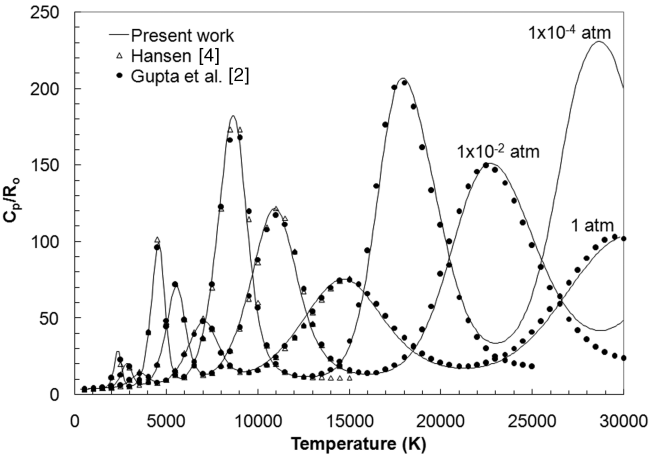

b) Nondimensional specific heat at constant pressure

Fig. 4 Comparison of the molecular-weight ratios and specific heat at constant pressure at various pressures.

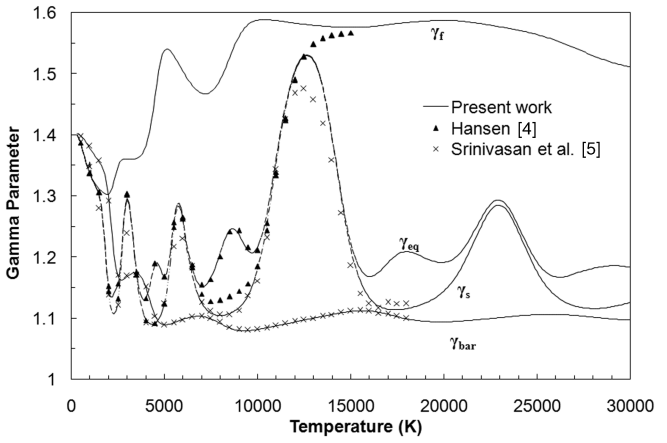

a) 1×10^{-4} atm

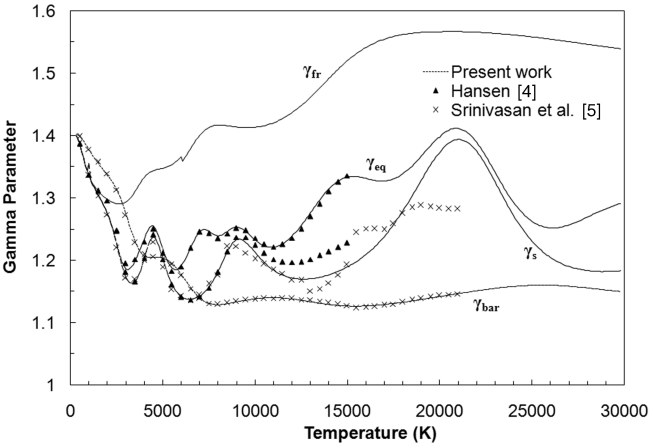

b) 1 atm

Fig. 5 Gamma parameters; lines are for results from this work.

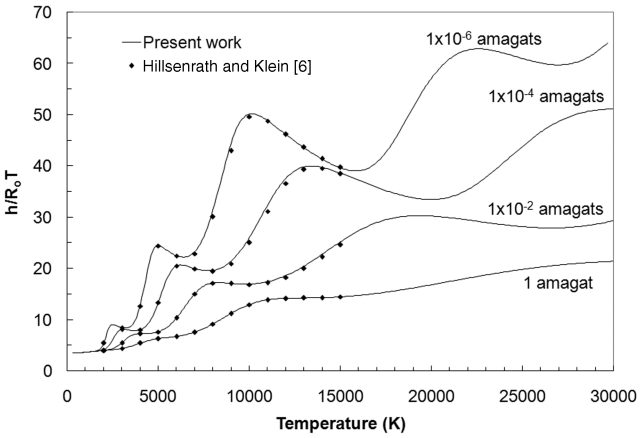

a) Nondimensional enthalpy

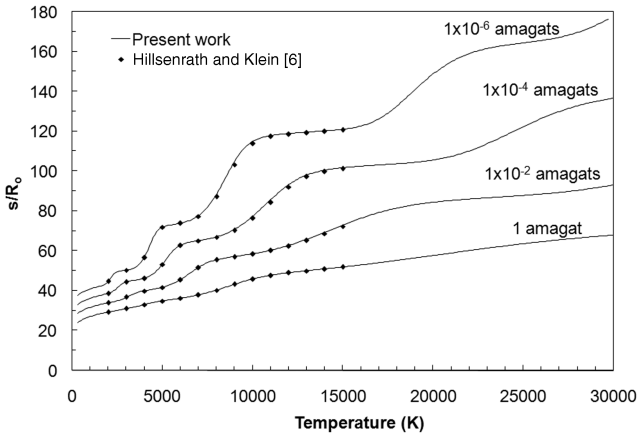

b) Nondimensional entropy

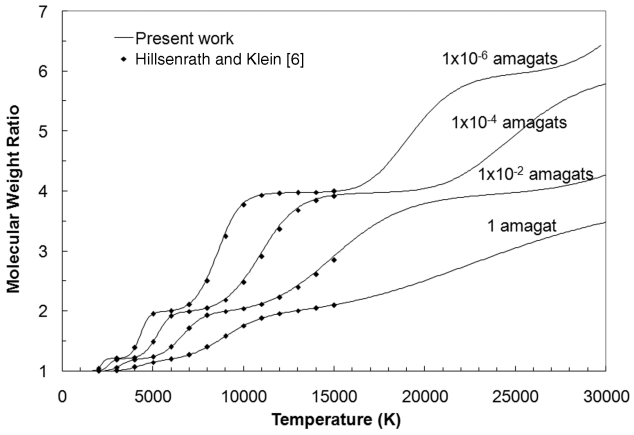

c) Molecular weight ratio

Fig. 6 Comparison of thermodynamic property results from this work to those of Hillensrath and Klein [6] results.

Figure 6 shows comparisons of the enthalpy, entropy, and molecular-weight ratio results of Hillensrath and Klein [6] with this work for densities of 1×10^{-6}, 1×10^{-4}, 1×10^{-2}, and 1 amagats, where an amagat is the density divided by the density of air at sea level. Excellent agreement between the thermodynamic results of Hillensrath and Klein and this work are obtained for all the densities of interest.

VII. Conclusions

It was found that composition results and the thermodynamic property results from this work compare well with results determined by Gupta et al. [2], Boulos et al. [3], Hansen [4], Srinivasan et al. [5], and Hillsenrath and Klein [6]. Because of the lack of higher ionization stages in these models, there are some differences at higher temperatures, especially for the lower-pressure cases. This work includes up to the third ionization stage, which is a higher number of ionization stages than other investigations have included. Some of the other models only include up to the first ions, whereas others include up to the second ions. For this reason, they limit the temperature range over which they present results. Results are presented in this paper up to 30,000 K for a number of pressures, with a focus on the lower pressures.

Acknowledgments

This work was funded in part through the Air Vehicles Directorate of the U.S. Air Force Research Laboratory managed byJames Miller, contract number F33615-02-C-3254. The authors would also like to thank the Dayton Area Graduate Studies Institute (DAGSI) for partial funding of this work.

References

[1] Strang, W., Tomaro, R., and Grismer, M., "The Defining Methods of Cobalt$_{60}$—A Parallel, Implicit, Unstructured Euler/Navier-Stokes Flow Solver," AIAA Paper 99-0786, 1999.

[2] Gupta, R. N., Lee, K.-P., Thompson, R. A., and Yos, J. M., "Calculation and Curve Fits of Thermodynamic and Transport Properties for Equilibrium Air to 30,000 K," NASA RP-1260, 1991.

[3] Boulos, M., Fauchaus, F., and Pfender, E., *Thermal Plasmas: Fundamentals and Applications*, Wiley, New York, 1994.

[4] Hansen, C., "Approximations for the Thermodynamic and Transport Properties of High-Temperature Air," NASA TR-R-50, 1959.

[5] Srinivasan, S., Tannehill, J., and Weilmuenster, K. J., "Simplified Curve Fits for the Thermodynamic Properties of Equilibrium Air," NASA RP-1181, 1987.

[6] Hillensrath, J., and Klein, M., "Tables of Thermodynamic Properties of Air in Chemical Equilibrium Including Second Virial Corrections from 1500 K to 15000 K," Arnold Engineering Development Center TR-65-58, Arnold AFB, TN, 1965.

[7] McBride, B., and Gordon, S., "Computer Program for Calculating and Fitting Thermodynamic Functions," NASA RP-1271, 1992.

[8] Gordon, S., and McBride, B., "Computer Program for Calculation of Complex Chemical Equilibrium Compositions and Applications 1: Analysis," NASA RP-1311, 1994.

[9] Gordon, S., "Complex Chemical Equilibrium Calculations," *Kinetics and Thermodynamics of High-Temperature Gases*, NASA SP-239, NASA, Washington, D. C., 1970, pp. 1–15.

[10] Reynolds, W. C., *The Element Potential Method for Chemical Equilibrium Analysis: Implementation in the Interactive Program STANJAN*, Dept. of Mechanical Engineering, Stanford Univ., Stanford, CA, 1986.

[11] Bottin, B., *PEGASE 4.4—Perfect Gas Equation for Arbitrary Mixtures at Low Pressure and High Temperatures*, Von Karman Inst. for Fluid Dynamics, Manual 47, Rhode St. Genèse, Belgium, 1997.

[12] Anderson, J. D., *Hypersonic and High Temperature Gas Dynamics*, McGraw–Hill, New York, 1989.
[13] Vincenti, W. G., and Kruger, C. H., *Introduction to Physical Gas Dynamics*, Wiley, New York, 1965.
[14] Smith, W. R., and Missen, R. W., *Chemical Reaction Equilibrium Analysis*, Wiley, New York, 1982.
[15] Colonna, G., *Computer Physics Communications*, Vol. 177, No. 6, 2007, pp. 493–499.
doi:10.1016/j.cpc.2007.01.012
[16] CANTERA, Software Package, Ver. 1.5, SourceForge, Inc., Mountain View, CA.
[17] CHEMKIN-II, Software Package, Sandia National Labs., Albuquerque, NM.
[18] McBride, B., and Gordon, S., "NASA Glenn Coefficients for Calculating Thermodynamic Properties of Individual Species," NASA TP-2002-211556, 2002.
[19] Gordon, S., and McBride, B., "Thermodynamic Data to 20,000 K for Monoatomic Gases, NASA TP-1999-208523, 1999.
[20] *Chemical Equilibrium with Applications* [online database], http://cea.grc.nasa.gov [retrieved June 2007].
[21] Goodwin, D., *Defining Phases and Interfaces: CANTERA 1.5*, Div. of Engineering and Applied Science, California Inst. of Technology, Pasadena, CA, 2003.
[22] Carey, V. P., *Statistical Thermodynamics and Microscale Thermophysics*, Cambridge Univ. Press, Cambridge, England, U.K., 1999.
[23] *NIST Atomic Spectra Database* [online database], http://physics.nist.gov/PhysRefData/ASD/index.html [retrieved June 2007].
[24] Capitelli, M., Colonna, G., Giordano, D., Marraffa, L., Casavola, A., Minelli, P., Pagano, D., Pietanza, L., and Taccogna, F., "High-Temperature Thermodynamic Properties of Mars Atmosphere Components," AIAA Paper 2004-2378, 2004.
[25] Bottin, B., "Thermodynamic Properties of Arbitrary Perfect Gas Mixtures at Low Pressures and High Temperatures," *Progress in Aerospace Sciences*, Vol. 36, No. 7, 2000, pp. 547–579.
doi:10.1016/S0376-0421(00)00009-9